Modeling Continuous Vinyl Acetate Emulsion Polymerization Reactions in a Pulsed Sieve Plate Column

ARTICLE *in* INDUSTRIAL & ENGINEERING CHEMISTRY RESEARCH · APRIL 2002

Impact Factor: 2.59 · DOI: 10.1021/ie010675q

3 AUTHORS:

Claudia Sayer
Federal University of Santa Catarina
109 PUBLICATIONS **948** CITATIONS
SEE PROFILE

Mauri Sergio Alves Palma
University of São Paulo
28 PUBLICATIONS **119** CITATIONS
SEE PROFILE

Reinaldo Giudici
University of São Paulo
120 PUBLICATIONS **1,055** CITATIONS
SEE PROFILE

Modeling Continuous Vinyl Acetate Emulsion Polymerization Reactions in a Pulsed Sieve Plate Column

Claudia Sayer, Mauri Palma, and Reinaldo Giudici*

Departamento de Engenharia Química, Escola Politécnica, Universidade de São Paulo, 05508-900 São Paulo, Brazil

A dynamic mathematical model is developed to simulate emulsion polymerization reactions carried out in a new type of reactor, the pulsed sieve plate column (PSPC). The PSPC is described by an axial dispersion model that allows one to cover the entire range between plug flow and perfectly mixed stirred tank reactors and, therefore, enables the simulation of a wide range of operational conditions. The developed model was validated with experimental data of vinyl acetate emulsion polymerization reactions. Besides presentation of a good agreement with experimental data at reactor start-up and at steady-state conditions, simulation results also showed that, at the studied operational conditions, the homogeneous nucleation mechanism is very important in order to represent the polymer particle number increase observed experimentally along the reactor length. The developed model was also used to test different start-up procedures and reaction temperatures.

1. Introduction

Tubular continuous reactors combine the advantages of the continuous stirred reactors (CSTRs), such as avoiding batch-to-batch product differences, with the flexibility of the batch and semicontinuous reactors. Also, tubular reactors present much higher heat-transfer areas (higher area/volume ratios) than the tank reactors and, therefore, allow a more efficient temperature control, especially in the case of highly exothermic processes such as the polymerization reactions.

In the case of emulsion polymerization reactions, to prevent the emulsion destabilization and plugging of the tubular reactor, two approaches were presented in the literature: (1) usage of high recycle rates; (2) introduction of pulses. In the second approach, good local agitation might be combined with little backmixing, resulting in much higher monomer conversions and particle concentrations than those obtained in single CSTRs.[1] In addition, sustained oscillations in those variables due to renucleations that are often observed in CSTRs[2−6] or in continuous loop reactors[7] may be minimized or avoided.

Previous results of Palma et al.[8,9] showed that it is possible to achieve high conversions in rather low residence times in a new type of reactor, the pulsed sieve plate column (PSPC), assessing the economic viability of this kind of reactor to perform emulsion polymerization reactions.

Nevertheless, to provide a deeper comprehension of the complex mechanisms involved in emulsion polymerization reactions carried out in this kind of reactor, the development of detailed mathematical models is of major importance, besides being one of the most powerful tools for the optimization of the operational conditions. Unfortunately, the number of studies involving the mathematical modeling of emulsion polymerization reactions carried out in tubular reactors with axial dispersion is still quite reduced.

Lynch and Kiparissides[10] developed a dynamic model of styrene emulsion polymerization reactions carried out in a closed-loop tubular reactor to represent the experimental data of Rollin et al.[11] The model takes into account the micellar nucleation mechanism and particle coalescence and considers that the axial diffusion is negligible for monomer and polymer particles in the emulsion; therefore, the axial diffusion coefficient was present only in the initiator balance equation.

Paquet and Ray[12] and Mayer et al.[1] developed axial dispersion models of emulsion polymerization reactions performed in pulsed tubular reactors. Paquet and Ray[12] developed a dynamic model of methyl methacrylate emulsion polymerization reactions with a micellar nucleation mechanism, and Mayer et al.[1] developed a steady-state model of styrene emulsion polymerization reactions with a micellar nucleation mechanism. Neither of those two models considered the homogeneous nucleation and particle coagulation mechanisms.

In a previous work Sayer and Giudici[13] compared the performance of two different modeling approaches: a tanks-in-series model and an axial dispersion model, with the last one solved either by the method of lines or by the orthogonal collocation technique, for the simulation of styrene emulsion polymerization reactions performed in a pulsed tubular reactor. Both models were validated with experimental data taken from literature[14] showing a good agreement. For the solution of the axial dispersion model, the method of lines presented more robust results than the orthogonal collocation technique for the simulation of transient reaction periods that may lead to steep fronts such as reactor start-up or disturbances in the reactant flow rates.

The objective of this work is to develop a dynamic mathematical model of vinyl acetate emulsion polymerization reactions carried out in the new PSPC reactor. The emulsion polymerization model takes micellar and homogeneous nucleation and particle coalescence mechanisms into account. Also, because of the relatively high solubility of vinyl acetate in the aqueous phase, the developed model takes account of the aqueous phase events that govern radical entry into polymer particles.

* To whom correspondence should be addressed. Fax: 55 11 38132380. E-mail: rgiudici@usp.br.

10.1021/ie010675q CCC: $22.00
Published on Web 00/00/0000 **PAGE EST: 11.7**

Table 1. Formulation: Vinyl Acetate Emulsion Polymerization Reactions

variable	mass fraction
monomer: vinyl acetate	0.1878
water	0.8062
emulsifier: sodium dodecyl sulfate	0.0024
initiator: sodium persulfate	0.0029
pH buffer: sodium carbonate	0.0007

Therefore, two different critical radical lengths were used as proposed by Gilbert:[15] one that specifies the critical degree of polymerization for radical entry into micelles and polymer particles (j_z) and another that specifies the critical degree of polymerization for homogeneous nucleation (j_{crit}). Danckwerts'[16] boundary conditions were used in the dynamic axial dispersion model of the PSPC. The method of lines was used to discretize the second-order partial differential equations along the axial direction. The model was capable of reproducing experimental data and provided a feasible explanation on the possible nucleation mechanism during vinyl acetate emulsion polymerization reactions carried out in the PSPC reactor. The developed model was also used to test different reaction temperatures and start-up procedures. According to Lu and Brooks[17] and Abad et al.,[18] who studied experimentally the effect of using different start-up procedures in vinyl acetate emulsion polymerization reactions performed in a continuous reactor and in vinyl acetate/Veova 10 emulsion copolymerization reactions performed in a continuous loop reactor, the start-up procedure might affect substantially the smoothness of the operation.

2. Experimental Section

2.1. Reactants. Distilled water was used in all polymerizations. The monomer (vinyl acetate), emulsifier (sodium dodecyl sulfate), initiator (sodium sulfate), and pH buffer (sodium carbonate) were used as supplied without further purification.

2.2. Batch Reactions in a Stirred Tank Reactor. Batch reactions were carried out at 50 and 55 °C using the recipe given in Table 1 in a 600 mL jacketed stirred tank glass reactor. To remove traces of dissolved oxygen, nitrogen was continuously bubbled into the reactor. Also the initial reactor charge, without the initiator, was purged with nitrogen for a period of 20 min at reaction temperature.

2.3. Continuous Reactions in the PSPC. The experimental setup for the continuous reactions comprises a PSPC composed of 5 stainless steel sections, each one with 1000 mm length and 40.0 mm internal diameter and each with its own independent jacket. The plates are stainless steel disks, each one with 39 holes of 3 mm in triangular arrangement, resulting in a free area of 22.3% in each plate. Plate spacing was 50 mm, resulting in a free volume of 95.7% of the reactor. The pulsator is composed of a piston that is connected to the bottom of the column by a bellows; the piston is connected through a rod to the eccentric of a rotor whose rotation generates a sinusoidal movement of the piston. The stroke length and the frequency can be adjusted respectively within the ranges 5−25 mm and 0.2−3.5 s^{-1}. At the upper part of the reactor, after the last reactor section and the last sampling point, the reaction medium continues to flow through a glass tube with overflow. This ensures that the jacketed reactor sections and the sampling points are always full. Figure 1 shows a schematic presentation of the continuous reactor used in this experimental procedure.

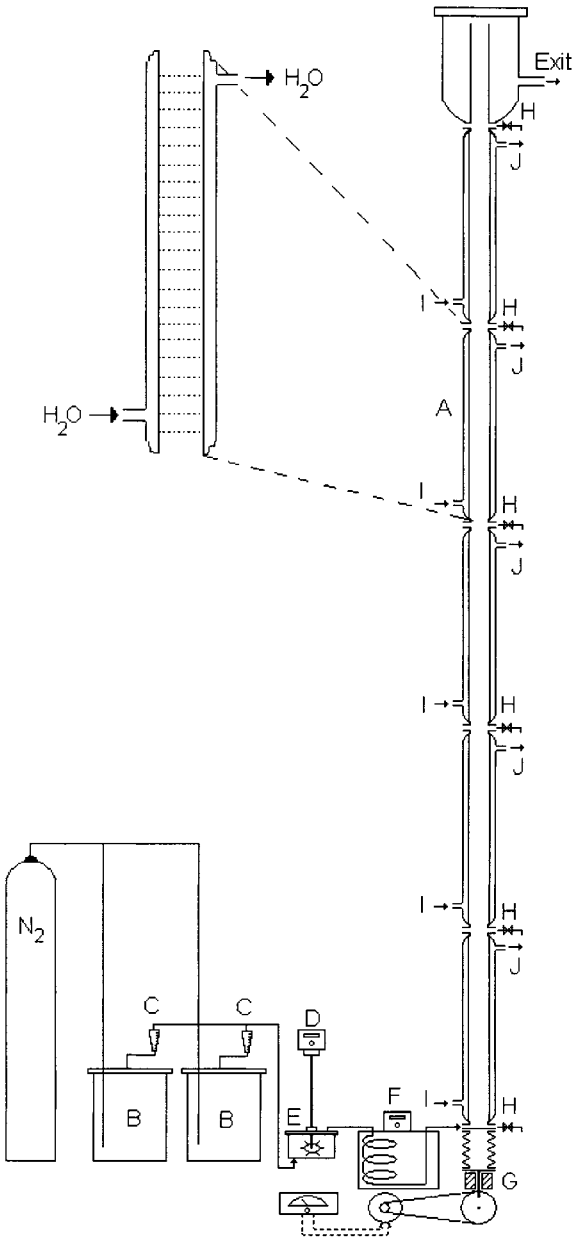

Figure 1. Schematic of experimental setup: A, PSPC; B, feeding tanks; C, rotameters; D, impeller; E, premixer; F, preheater; G, pulsator; H, sampling points; I, jacket inlets; J, jacket outlets.

The startup procedure in the reactions was comprised of filling the reactor with water and heating to the reaction temperature (55 °C). The pulsator was then turned on, and the reactants were fed in two different streams: (1) an aqueous solution of emulsifier (sodium dodecyl sulfate), initiator (sodium persulfate), and pH buffer (sodium carbonate) and (2) an organic phase consisting of the commercial grade monomer (vinyl acetate). Those two streams are pre-emulsified together in a small premixer before entering the reactor. To remove traces of dissolved oxygen, nitrogen was continuously bubbled into both feed tanks. Tables 1 and 2 show the formulation and the experimental conditions.

To allow a better understanding of the complex mechanisms involved in these kinds of reactions, samples were taken both at the reactor outlet and at five other sampling points evenly distributed along the reactor.

Table 2. Experimental Conditions: Vinyl Acetate Emulsion Polymerization Reactions in the PSPC

variable	run 1	run 2	run 4	run 5
temperature (°C)	55.0	55.0	55.0	55.0
residence time (min)	30.0	30.0	60.0	60.0
stroke length (mm)	5.0	15.0	5.0	15.0
pulsation frequency (s^{-1})	3.5	3.5	3.5	3.5
Peclet number[a]	92.0	62.0	92.0	40.0

[a] Peclet numbers from pulse tracer studies.[19]

2.4. Latex Characterization. Monomer conversion was measured by gravimetry, and the particle diameter was measured by photon correlation spectroscopy (Malvern Zetasizer S). When extremely low polymer particle concentrations are used, as required by photon correlation spectroscopy, the monomer in the polymer particles completely diffuses from the polymer particles to the aqueous phase, and so the measured diameter corresponds to the average diameter of the unswollen polymer particles. No monomer droplets separation procedure was required in advance of the average particle diameter measurements because the samples were taken at high enough conversions to avoid the presence of monomer droplets. The particle concentration was computed from conversion and average particle diameter data.

3. Model Development

3.1. Emulsion Polymerization Modeling. The mathematical model of emulsion polymerization reactions used in this work was based on previous models developed by Casella,[20] Sayer et al.,[21] and Araújo et al.[7] respectively of batch, semicontinuous, and continuous loop reactors. The following assumptions are used to derive the model equations:

(i) Monomer concentrations in polymer particles, monomer droplets, and the aqueous phase are at thermodynamic equilibrium.

(ii) The total mass of polymer produced in the aqueous phase is negligible.

(iii) Particle nucleation occurs through the micellar and homogeneous mechanisms.

(iv) Particle coagulation depends on the initiator concentration.

(v) Polymer particles are spherical and monodisperse.

(vi) The critical micellar concentration (cmc) and the surface covered by 1 mol of emulsifier are constant.

(vii) The gel effect is negligible for vinyl acetate emulsion polymerization reactions.

(viii) The pseudo-steady-state assumption is valid for polymer radicals.

(ix) Kinetic constants do not depend on the chain length.

(x) Kinetic constants in the aqueous and polymer phases are the same.

(xi) Radicals generated by initiation or chain transfer to monomer present similar reactivities.

(xii) Reactions are performed at constant temperature.

(xiii) Radial mixing is perfect.

(xiv) The average net forward velocity is constant.

(xv) Axial mixing is represented by an effective axial dispersion coefficient.

(xvi) The axial dispersion coefficient is the same for all phases present in the emulsion (continuous aqueous phase, micelles, polymer particles, and monomer droplets).

To model continuous reactions carried out in the PSPC, a dynamic axially dispersed plug-flow model was implemented. Given the previous assumptions, the population and mass balance equations for a continuous emulsion polymerization system are presented below:

(a) Polymer particle concentration N_p

$$\frac{\partial N_p}{\partial t} + v_z \frac{\partial N_p}{\partial z} - De \frac{\partial^2 N_p}{\partial z^2} = R_{mic} + R_{hom} - c_c N_p^2 \quad (1)$$

where De is the effective dispersion coefficient in cm^2/s that is determined from pulse tracer studies.[19] De and is used to compute the Peclet number (Pe) and v_z is the average net forward velocity:

$$Pe = v_z(a_{col}/De) \quad (2)$$

$$v_z = q_e/(\pi r_{col}^2 f_{void}) \quad (3)$$

where q_e is the inlet flow rate of the reactor in cm^3/s, r_{col} and a_{col} are respectively the radius and the length of the PSPC in cm, and f_{void} is the void fraction of the PSPC. R_{mic} and R_{hom} represent the micellar and homogeneous nucleation rates, and $c_c N_p^2$ represents the rate of particle coalescence.

Micellar Nucleation.

$$R_{mic} = k_{abs}^m R_{ent} N_{mic} \quad (4)$$

where R_{ent} is the concentration of radicals in the aqueous phase that may enter polymer particles, computed by eq 25, and k_{abs}^m is the absorption rate coefficient of radicals from the aqueous phase by the micelles given by the Smoluchowski equation:

$$k_{abs}^m = 4\pi D_w r_m N_a f_{abs}^m \quad (5)$$

where D_w, r_m, and f_{abs}^m represent respectively the diffusion coefficient in the aqueous phase, the radius of one micelle, and the absorption efficiency of radicals from the aqueous phase by the micelles.

Variable N_{mic} is the concentration of micelles formed when the emulsifier concentration in the aqueous phase $[E]^{aq}$ is above the critical micellar concentration:

$$N_{mic} = M_{mic}(v_{aq}/v_R) \quad (6)$$

where M_{mic} is the number of micelles per volume of the aqueous phase, computed by eq 11. v_R, v_p, and v_{aq} are respectively the volumes of the reactor and of the polymer and aqueous phases.

Homogeneous Nucleation.

$$R_{hom} = c_{hom}^0 k_p [M]_{aq} R_{jcrit} N_a (v_{aq}/v_R) \quad (7)$$

where c_{hom}^0 is the coefficient of homogeneous nucleation and $k_p[M]_{aq}$ is the propagation rate in the aqueous phase.

Variable R_{jcrit}, is the concentration of radicals presenting critical length j_{crit} in the aqueous phase, computed as described in section 3.1.1 (eq 24).

Particle Coalescence. To avoid using rather complex relations such as the extensions of the Derjaguin−Landau−Verwey−Overbeek (DLVO) model that involve a significant number of often unknown parameters,[7,15] a simple equation for the rate constant of particle

coalescence was used. This equation is an extremely simplified version of the DLVO model, and the only effect that is accounted for in this equation is the initiator concentration in the aqueous phase, because increasing the electrolyte concentrations enhances the particle coagulation rate:[22]

$$c_c = c_c^0 \sqrt{[I] v_R N_a} \tag{8}$$

where c_c^0 is the only unknown parameter that must be adjusted in order to represent experimental data.

(b) Initiator concentration in the reactor [I]:

$$\frac{\partial [I]}{\partial t} + v_z \frac{\partial [I]}{\partial z} - De \frac{\partial^2 [I]}{\partial z^2} = -[I] k_d \tag{9}$$

(c) Emulsifier concentration in the reactor [E]:

$$\frac{\partial [E]}{\partial t} + v_z \frac{\partial [E]}{\partial z} - De \frac{\partial^2 [E]}{\partial z^2} = 0 \tag{10}$$

In emulsion polymerization systems, the emulsifier might be present in three different ways: (a) free in the aqueous phase ($[E]^{aq}$); (b) in the form of micelles in the aqueous phase (M_{mic}); (c) adsorbed on polymer particles ($[E]_{ads}$) and monomer droplets. Because monomer droplets present significantly bigger radii than polymer particles, they present a much lower total superficial area and, therefore, the amount of emulsifier adsorbed on monomer droplets might be neglected:

$$[E] = \frac{[E]^{aq} v_{aq} + \gamma M_{mic} v_{aq} + a_p N_p [E]_{ads}}{v_R} \tag{11}$$

where $[E]^{aq}$ is the concentration of the emulsifier in the aqueous phase, γ is the number of moles of emulsifier per micelle, and $[E]_{ads}$ is the emulsifier adsorbed on polymer particles per unit surface. Variable γ is computed by

$$\gamma = 4\pi r_m^2 / a_s \tag{12}$$

where a_s is the area covered by 1 mol of emulsifier and a_p is the superficial area of one polymer particle swollen with monomer:

$$a_p = 4\pi r_p^2 \tag{13}$$

r_p is the radius of one polymer particle swollen with monomer, computed by

$$r_p = \sqrt[3]{(3 v_p / N_p v_R)/4\pi} \tag{14}$$

Variables $[E]^{aq}$, $[E]_{ads}$, and M_{mic} must be computed for three different situations: (a) if the emulsifier concentration is above the cmc ($[E]_{cmc}$), then the emulsifier concentration in the aqueous phase ($[E]^{aq}$) equals $[E]_{cmc}$, the emulsifier concentration adsorbed on polymer particles ($[E]_{ad}$) equals the saturation concentration ($[E]^{sat}_{ads} = 1/a_s$), and M_{mic} is computed with eq 11; (b) if the emulsifier concentration is below $[E]_{cmc}$ and the emulsifier concentration is enough to saturate polymer particles, then M_{mic} equals zero, $[E]_{ad}$ equals $[E]^{sat}_{ads}$ (assuming that the emulsifier is preferably absorbed on polymer particles rather than in the aqueous phase), and $[E]^{aq}$ is computed with eq 11; (c) if the emulsifier concentration is below $[E]_{cmc}$ and the emulsifier concentration is not enough to saturate polymer particles, then M_{mic} and $[E]^{aq}$ equal zero and $[E]_{ad}$ is computed with eq 11.

(d) Monomer concentration in the reactor [M]:

$$\frac{\partial [M]}{\partial t} + v_z \frac{\partial [M]}{\partial z} - De \frac{\partial^2 [M]}{\partial z^2} = -\frac{\bar{n} N_p}{N_a} (k_p [M]_p + k_f [M]_p) \tag{15}$$

$[M]_p$ is the monomer concentration in polymer particles. The computation of monomer concentrations in the different phases present in emulsion polymerization reactions was by the iterative procedure proposed by Omi et al.[23]

(e) Polymer mass in the reactor P:

$$\frac{\partial P}{\partial t} + v_z \frac{\partial P}{\partial z} - De \frac{\partial^2 P}{\partial z^2} = \frac{\bar{n} N_p}{N_a} k_p [M]_p P M_m \tag{16}$$

(f) Water fraction in the reactor ϕ_w:

$$\frac{\partial \phi_w}{\partial t} + v_z \frac{\partial \phi_w}{\partial z} - De \frac{\partial^2 \phi_w}{\partial z^2} = 0 \tag{17}$$

3.1.1. Computation of the Average Number of Radicals per Polymer Particle. The method proposed by Ugelstad et al.[24] was used for the iterative computation of the average number of radicals per polymer particle $\bar{n}$:

$$\bar{n} = \frac{1}{2} \cfrac{h^2/4}{m + 0 + \cfrac{h^2/4}{m + 1 + \cfrac{h^2/4}{m + 2 + \ldots}}} \tag{18}$$

where h and m are the relative absorption/termination and desorption/termination coefficients, defined as

$$h = \left(\frac{8 k_{abs} R_{ent} N_a v_p}{k_t x_{gel} N_p v_R} \right)^{1/2} \tag{19}$$

$$m = \frac{k N_a v_p}{k_t x_{gel} N_p v_R} \tag{20}$$

k_{abs} is the coefficient of the absorption rate of radicals from the aqueous phase by the polymer particles given by the Smoluchowski equation:

$$k_{abs} = 4\pi D_w r_p N_a f_{abs} \tag{21}$$

where R_{ent} is the concentration of radicals in the aqueous phase that may enter polymer particles. R_{ent} is computed by the iterative procedure developed by Araújo[25] based on the existence of two different critical radical lengths as proposed by Gilbert:[15] one that specifies the critical degree of polymerization for radical entry into micelles and polymer particles (j_z) and another that specifies the critical degree of polymerization for homogeneous nucleation (j_{crit}):

$$\Psi = k_p [M]_{aq} + k_{abs} \frac{N_p v_R}{v_{aq} N_a} + k_{abs}^m \frac{N_{mic} v_R}{v_{aq} N_a} + k_t R_{aq} \tag{22}$$

$$R_1 = \left(\frac{2Iv_R f k_d}{v_{aq}} + \frac{k\bar{n}N_p v_R}{v_{aq}N_a} \right) \Bigg/ \left(k_p[M]_{aq} + k_t R_{aq} \right) \quad (23)$$

$$R_{j_{crit}} = R_1 \left(\frac{k_p[M]_{aq}}{k_p[M]_{aq} + k_t R_{aq}} \right)^{j_z - 2} \left(\frac{k_p[M]_{aq}}{\Psi} \right)^{j_{crit} - j_z} \quad (24)$$

$$R_{ent} = R_1 \left(\frac{k_p[M]_{aq}}{k_p[M]_{aq} + k_t R_{aq}} \right)^{j_z - 2} \sum_{j=j_z}^{j_{crit}-1} \left(\frac{k_p[M]_{aq}}{\Psi} \right)^{j - j_z + 1} \quad (25)$$

$$R_{aq} = R_1 \left[1 + \sum_{j=2}^{j_z - 1} \left(\frac{k_p[M]_{aq}}{k_p[M]_{aq} + k_t R_{aq}} \right)^{j-1} \right] + R_{ent} \quad (26)$$

where R_{aq} is the concentration of radicals in the aqueous phase, j_z and j_{crit} are the critical lengths for radical entry into micelles and polymer particles and for homogeneous nucleation,[15] which depend on the solubility of the monomer in the aqueous phase, $k_t R_{aq}$ and $k_p[M]_{aq}$ are termination and propagation rates in the aqueous phase per unit radical, f is the efficiency of forming radicals by the decomposition of the initiator, and k is the coefficient of the desorption rate of radicals from polymer particles:[26,27]

$$k = k_f[M]_p \frac{k_{0m}}{(k_{0m}\beta_m + k_p[M]_p)} \quad (27)$$

where k_{0m} and β_m are the exit rate of a monomeric radical from a polymer particle and the probability of a radical in the aqueous phase to react by propagation or by termination:

$$k_{0m} = \frac{3\dfrac{D_w}{r_p{}^2 k_m{}^p}}{2\dfrac{D_w}{D_p k_m{}^p} + 1} \quad (28)$$

$$\beta_m = \frac{k_p[M]_{aq} + k_t R_{aq}}{\Psi} \quad (29)$$

where D_p is the diffusion coefficient of a radical in polymer particles in cm^2/s.

3.2. Solution of the Axial Dispersion Model. The boundary conditions of Danckwerts,[16] eqs 31 and 32, have been applied to the dynamic axial dispersion model, represented here by the vector form (30):

$$\frac{\partial x}{\partial t} + v_z \frac{\partial x}{\partial z} - De \frac{\partial^2 x}{\partial z^2} = -\text{Rate}_{\text{consumption}} + \text{Rate}_{\text{generation}} \quad (30)$$

$$\frac{De}{v_z} \frac{dx}{dz} = x - x_e \qquad z = 0 \qquad \forall\, t \quad (31)$$

$$\frac{dx}{dz} = 0 \qquad z = 1 \qquad \forall\, t \quad (32)$$

where x is the vector of state variables (eqs 1, 9, 10, and 15−17) and z is the dimensionless reactor length.

The method of lines was used to solve the second-order partial differential equations. By this procedure the partial differential equations, eq 30, are discretized by the finite differences technique; consequently, the balance equations are transformed into ordinary differential equations, eq 33, and the boundary conditions, eqs 31 and 32, are transformed into algebraic equations, eqs 34 and 35:

$$\frac{dx_i}{dt} = \left[De \left(\frac{x_{i-1} - 2x_i + x_{i+1}}{\Delta z^2} \right) - v_z \left(\frac{x_{i+1} - x_{i-1}}{2\Delta z} \right) \right] - \text{Rate}_{\text{consumption}_i} + \text{Rate}_{\text{generation}_i} \quad (33)$$

with the following boundary conditions:

$$x_1 = \frac{4x_2 - x_3 + 2\Delta z \dfrac{v_z}{De} x_e}{2\Delta z \dfrac{v_z}{De} + 3} \quad (34)$$

$$x_{ND+2} = \frac{4x_{ND+1} - x_{ND}}{3} \quad (35)$$

where ND is the number of internal points and Δz is the length between two discretization points:

$$\Delta z = \frac{1}{ND + 1} \quad (36)$$

The developed model was implemented in FORTRAN, and the system of differential algebraic equations is solved by the solver DASSL.[28] This integrator uses the backward differentiation formulas to solve implicit differential algebraic systems. All simulations were performed using 40 evenly spaced internal nodes along the axial direction.

4. Results and Discussion

To validate the kinetic model at first the model was used for the simulation of batch vinyl acetate emulsion polymerization reactions performed at 50 and 55 °C. For those simulations the terms related with the axial velocity and with the axial dispersion of the mass balance equations (second and third terms in eq 30) were set equal to zero. Simulation results were compared with experimental data of Palma et al.[29] of batch reactions carried out with exactly the same formulation as that used in the reactions in the PSPC presented in Table 1. Kinetic constants and other parameters used in the following simulations are presented in Table 3. Some parameters related to micellar and homogeneous particle nucleation and to particle coalescence were estimated based on the results of several reactions performed in a stirred tank batch reactor and in the PSPC. It is important to say that the only "unknown" parameter that distinguishes the model of the batch reactions from that of the reactions in the PSPC is the Peclet number that was measured experimentally by previous tracer studies performed in the PSPC.[19]

Figures 2 and 3 compare simulation and experimental conversion and average particle diameter results of batch vinyl acetate emulsion polymerization reactions, and a fairly good agreement might be observed. Because the radical initiation rate and the propagation rate increase with increasing temperatures, higher reaction temperatures lead to higher reaction rates and to a faster achievement of the final conversions.

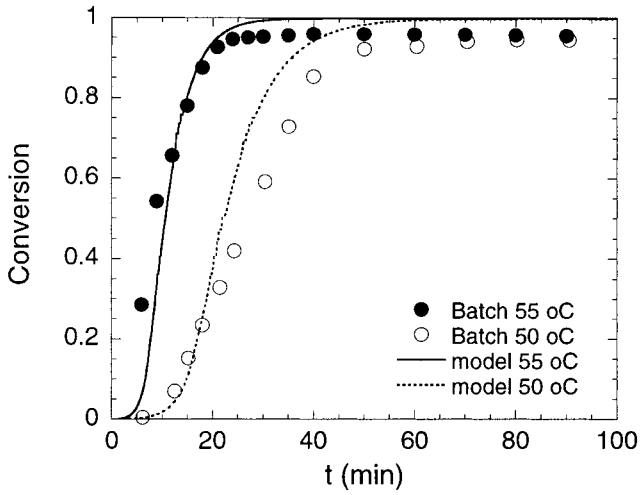

Figure 2. Evolution of conversion during batch vinyl acetate emulsion polymerization reactions. Comparison between experimental and simulation results.

Table 3. Parameters Used in the Simulations (Vinyl Acetate)

param	value	units	ref
k_d	$1.8 \times 10^{17} \exp(-34100/RT)$	s^{-1}	4
k_p	$1.44544 \times 10^{10} \times \exp(-2489.65/T)$	$cm^3/mol{\cdot}s$	30
k_f	$2.43 \times 10^{-5} k_{pAA}$	$cm^3/mol{\cdot}s$	31
k_t	$5.255 \times 10^{9} \exp(-884/T)$	$cm^3/mol{\cdot}s$	32
a_s	$57 \times 10^{-16} N_a$	cm^2/mol	33
r_m	2.5×10^{-7}	cm	33
$[E]_{cmc}$	2.43×10^{-6}	mol/cm^3	34
D_W	1.1×10^{-5}	cm^2/s	33
D_p	1.1×10^{-6}	cm^2/s	33
f	1.0		12
f_{abs}	3.3×10^{-3}		adjusted in this work
f_{abs}^m	1.0×10^{-5}		adjusted in this work
c_c^0	4.0×10^{-26}	cm^3/s	adjusted in this work
c_{hom}^0	3.0×10^{-3}		adjusted in this work
j_{crit}	16		15
j_z	8		15
PM_E	288.38	g/mol	35
PM_w	18.01	g/mol	36
ρ_m	0.933	g/cm^3	35
ρ_p	1.13	g/cm^3	7
ρ_w	1.028	g/cm^3	36
k_m^d	34.7		37
k_m^p	29.5		37

In the next figures simulation results are compared with experimental data of a continuous vinyl acetate emulsion polymerization reaction carried out in the PSPC. Figures 4−6 present the dynamic behavior during reactor start-up. In Figure 4 it might be observed that the polymer fraction in the reactor increases quite abruptly and that less than two residence times are required to reach steady-state conditions (residence time = 30 min). This behavior is in accordance with the low axial dispersion conditions of this reaction (Pe = 92). Figures 5 and 6 compare experimental and simulated particle concentrations and average particle diameters. The experimental particle concentration (Figure 5) shows a quite complex behavior during reactor start-up. The initial overshoot in the particle concentration may be explained by the axial dispersion in the PSPC because it affects the concentrations of reactants and polymer particles along the reactor and, consequently,

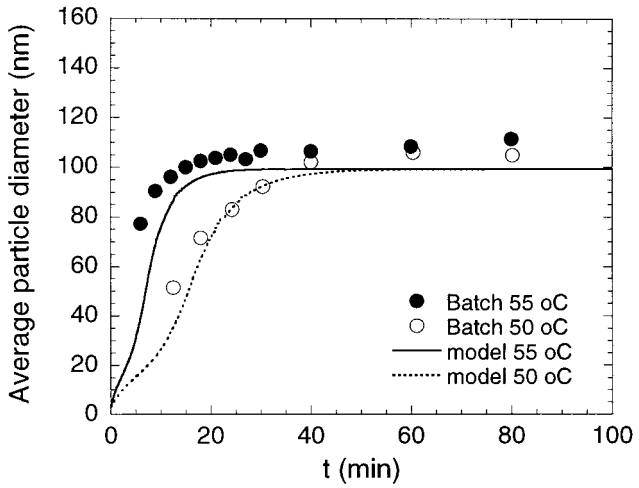

Figure 3. Evolution of average particle diameter during batch vinyl acetate emulsion polymerization reaction. Comparison between experimental and simulation results.

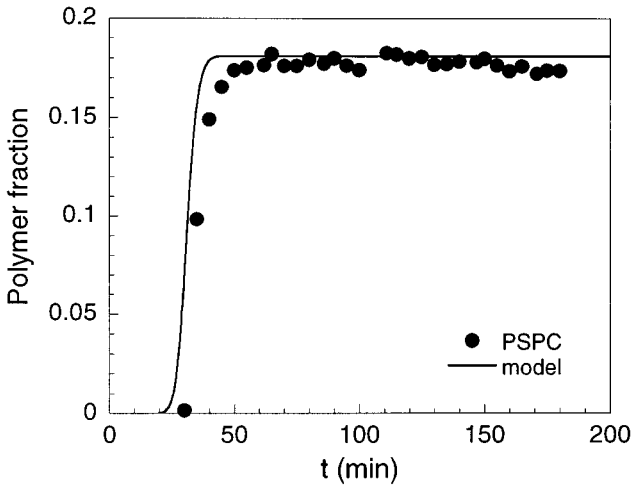

Figure 4. Evolution of polymer fraction during a continuous vinyl acetate emulsion polymerization reaction in the PSPC. Comparison between experimental and simulation results.

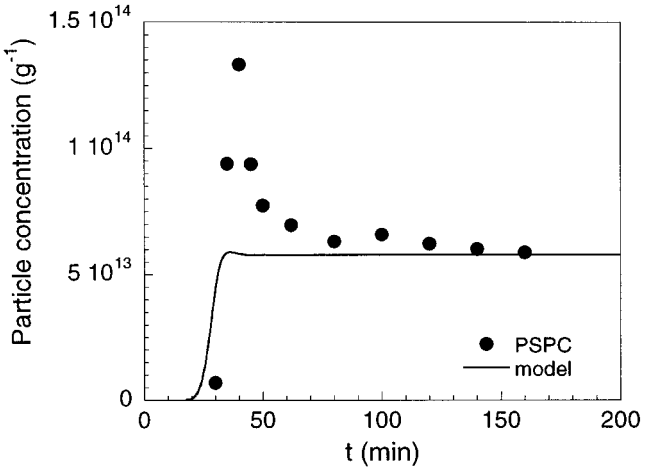

Figure 5. Evolution of particle concentration during a continuous vinyl acetate emulsion polymerization reaction in the PSPC. Comparison between experimental and simulation results.

particle nucleation. During the start-up procedure, the reactor is filled only with water; therefore, a significant fraction of the available radicals, emulsifier, and monomer is used to nucleate new particles. On the other hand, at the steady state, previously formed polymer

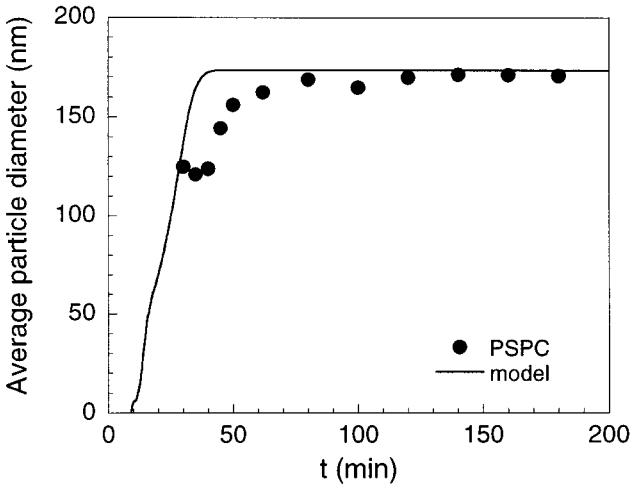

Figure 6. Evolution of average particle diameter during a continuous vinyl acetate emulsion polymerization reaction in the PSPC. Comparison between experimental and simulation results.

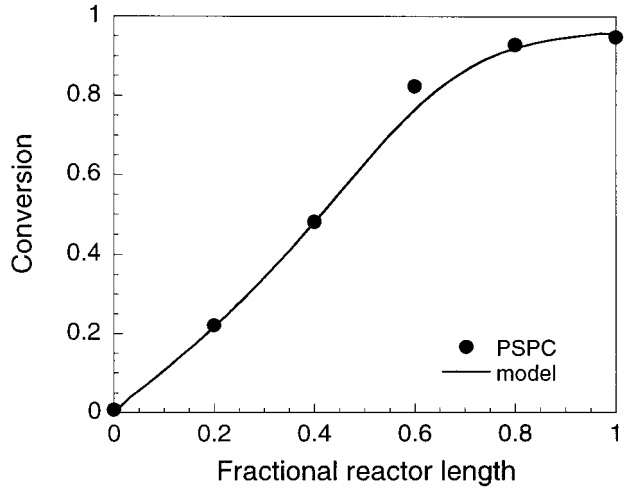

Figure 7. Evolution of conversion along the reactor length in a continuous vinyl acetate emulsion polymerization reaction in the PSPC. Comparison between experimental and simulation steady-state results.

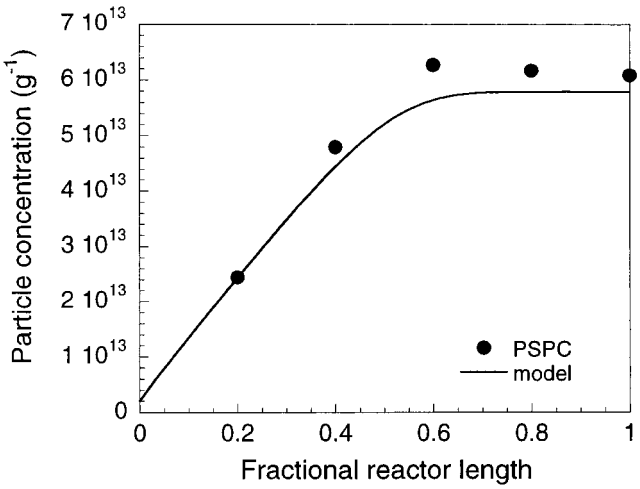

Figure 8. Evolution of particle concentration along the reactor length in a continuous vinyl acetate emulsion polymerization reaction in the PSPC. Comparison between experimental and simulation steady-state results.

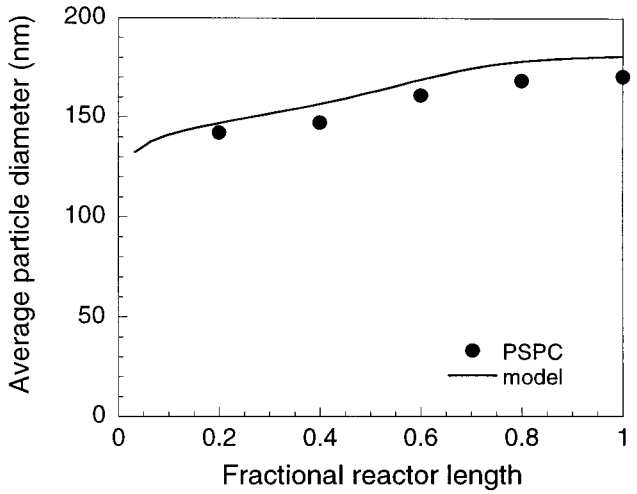

Figure 9. Evolution of average particle diameter along the reactor length in a continuous vinyl acetate emulsion polymerization reaction in the PSPC. Comparison between experimental and simulation steady-state results.

particles capture part of the available radicals, emulsifier, and monomer. As a consequence, at steady-state conditions, less radicals, emulsifier, and monomer are available in the aqueous phase to nucleate new particles; this explains the decrease of the particle concentration when the steady state is achieved. This is also the reason why much lower particle concentrations are obtained in the PSPC ($N_p/g \cong 6 \times 10^{13}$ g^{-1}; $D_p \cong 170$ nm) than in the batch reactions ($N_p/g \cong 2 \times 10^{14}$ g^{-1}; $D_p \cong 110$ nm) for similar residence times. The mathematical model was able to represent the dynamic and steady-state trends along the PSPC. Nevertheless, despite considering micellar and homogeneous nucleation and particle coalescence mechanisms, the model was not able to represent exactly a complex behavior observed in this reaction, the magnitude of the initial particle concentration overshoot (Figure 5). This might be attributed to the monodisperse particles assumption, as observed by Araújo et al.[7] Another important factor is the difficulty of predicting which mechanism (micellar and homogeneous nucleation and particle coalescence) is operative in each particular reaction instant.[15,38]

Figure 7 presents the evolution of monomer conversion along the fractional reactor length. Results show that it is possible to achieve high conversions in short residence times, 30 min, in the PSPC. Figures 8 and 9 present the evolution of the average particle diameter and particle concentration along the fractional reactor length. Agreement between experimental data and simulation results is quite good. An interesting aspect observed in Figure 9 is that, despite the relatively low emulsifier concentration used in these reactions (~1.24 $\times$ 10^{-5} mol/cm^3 of water), the particle concentration increases along more than half of the reactor length. As shown by the simulation results presented in Figures 10 and 11, this increase might be attributed to significant homogeneous nucleation occurring almost along the whole reactor length, while the micellar nucleation mechanism is limited to the region near the reactor entrance. Figure 12 presents the simulated emulsifier concentration in the aqueous phase during reactor start-up along the fractional reactor length. It might be observed that the emulsifier concentration in the aqueous phase reaches the cmc only in the region near the reactor entrance. After the reactor entrance, the emulsifier concentration in the aqueous phase increases during start-up, reaching a maximum, which is below the cmc,

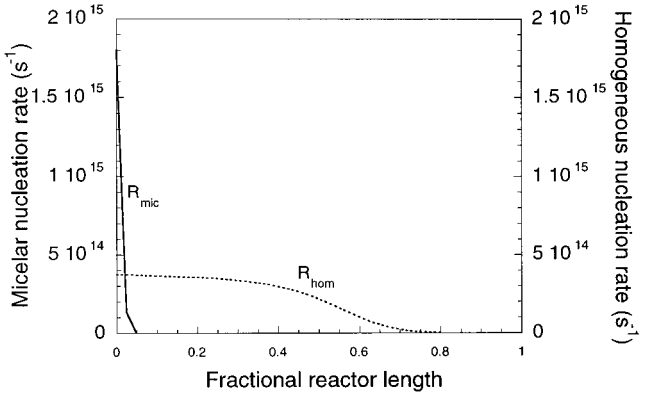

Figure 10. Evolution of micellar and homogeneous nucleation rates along the reactor length in a continuous vinyl acetate emulsion polymerization reaction in the PSPC. Simulation steady-state results.

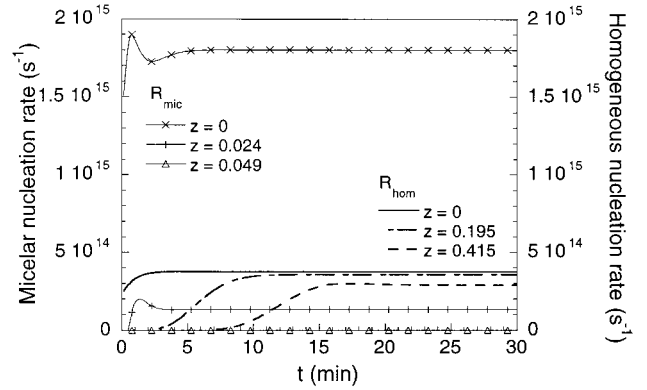

Figure 11. Evolution of micellar and homogeneous nucleation rates along the reactor length during the first residence time of a continuous vinyl acetate emulsion polymerization reaction in the PSPC. Simulation results.

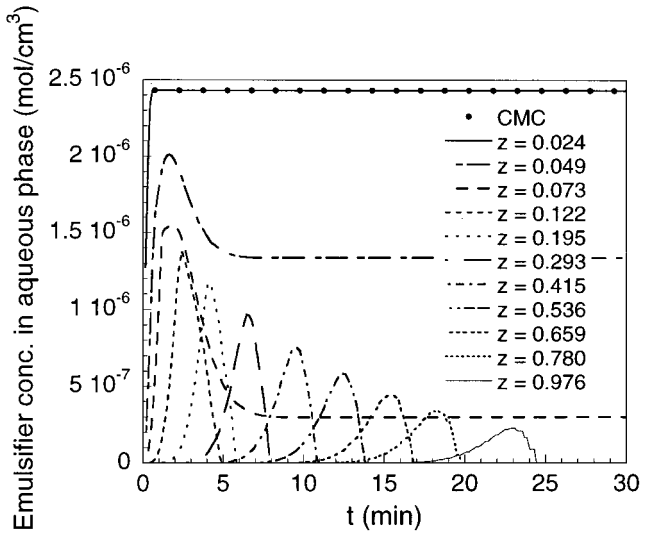

Figure 12. Evolution of emulsifier concentration in the aqueous phase along the reactor length during the first residence time of a continuous vinyl acetate emulsion polymerization reaction in the PSPC. Simulation results.

and then decreases as the emulsifier is used to stabilize polymer particles.

Figure 13 compares the evolution of monomer conversion along the fractional reactor length of several reactions (runs 1, 2, 4, and 5). As presented in Table 2, runs 1 and 2 were carried out with a residence time of

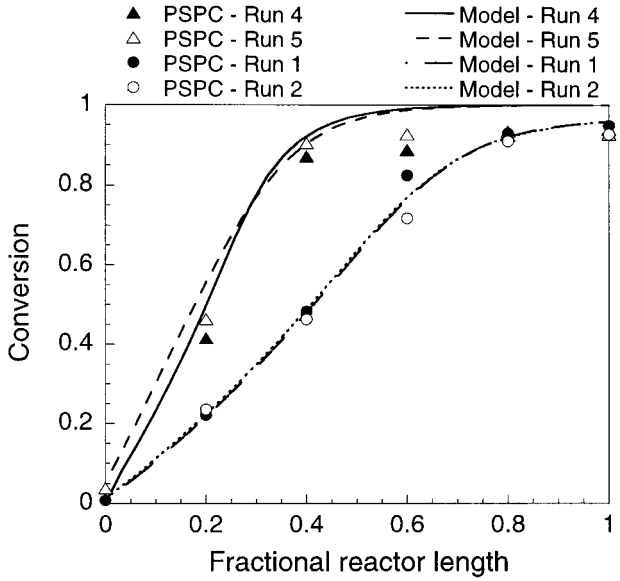

Figure 13. Comparison of the evolution of conversion along the reactor length in continuous vinyl acetate emulsion polymerization reactions in the PSPC with different residence times and Peclet numbers. Steady-state results.

30 min and runs 4 and 5 with a residence time of 60 min. Another difference among those reactions is the Peclet number: runs 1 and 2 respectively with $Pe = 92$ and 62 and runs 4 and 5 respectively with $Pe = 92$ and 40. Results show that while in runs 4 and 5 final conversions are achieved in the first half of the reactor, in runs 1 and 2 conversions increase smoothly along the whole reactor length, reaching exactly the same final value (above 95%). Although the effect of the differences in the Peclet number are hardly noticed in the experimental data, they might be observed in the simulation results of runs 4 and 5 because those reactions presented a more significant difference in the Peclet numbers. Compared to run 4, run 5 shows a higher conversion at the reactor entrance, but the final conversion is achieved later. This behavior is in agreement with the higher axial mixing of run 5. The model was able to represent the effect of the residence time.

Despite not being able to represent exactly the magnitude of the initial particle concentration overshoot, the model is able to predict accurately the steady-state behavior and important dynamic trends. Therefore, the developed model is believed to be a useful tool to complement experimental results and to perform simulations in advance of carrying out reactions under new operational conditions. In sequence the model is used to compare different reaction temperatures and several different start-up procedures.

Figures 14 and 15 compare the behavior of reactions performed at three different temperatures (50, 55, and 60 °C). In Figure 14a it might be observed that at 50 °C, because of the lower reaction rates (initiation and propagation rates), the final polymer fraction is much lower than that in the reaction at 55 or 60 °C. This result is in agreement with the result of the batch reaction at 50 °C (Figure 2); that at 30 min (residence time used in the PSPC) presented a conversion of around 50%. Increasing the reaction temperature from 55 to 60 °C resulted in only a slight increase in the polymer fraction, because the final conversion at 55 °C was already above 95% (as might be observed in Figure

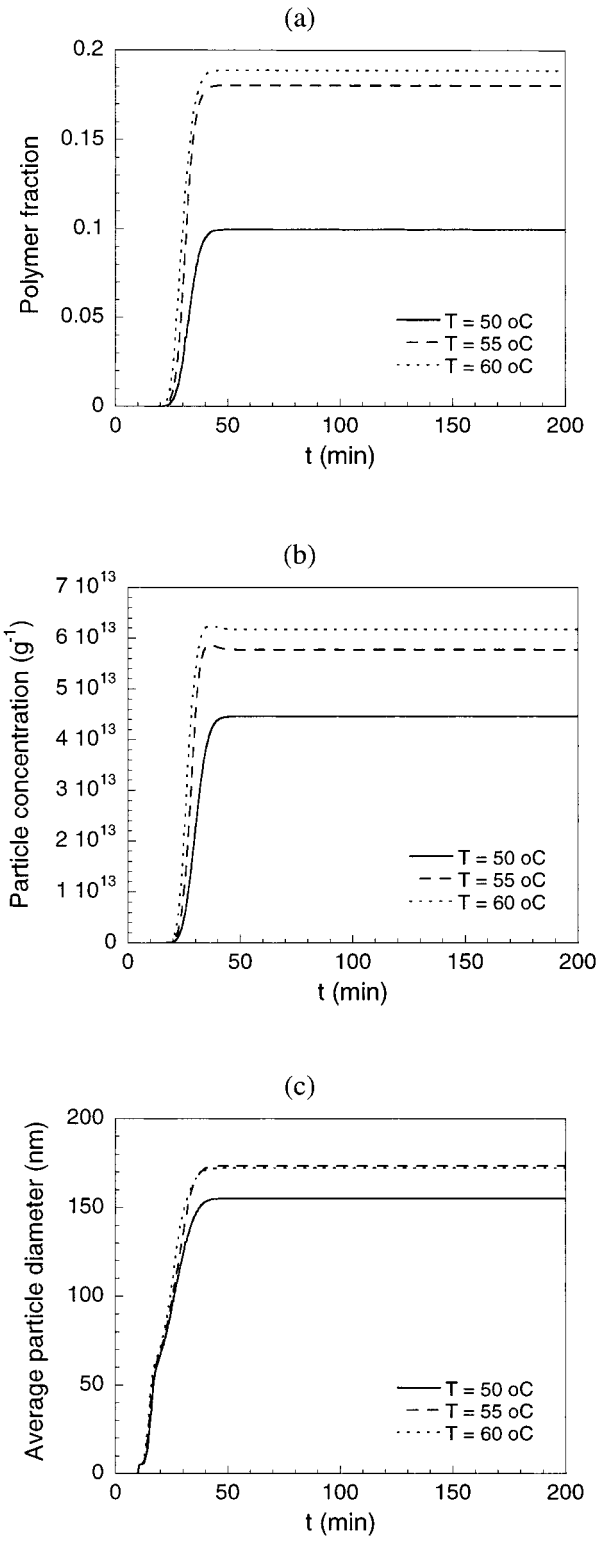

Figure 14. Effect of reaction temperature on the dynamic behavior of continuous vinyl acetate emulsion polymerization reaction in the PSPC: (a) conversion; (b) particle concentration; (c) average particle diameter.

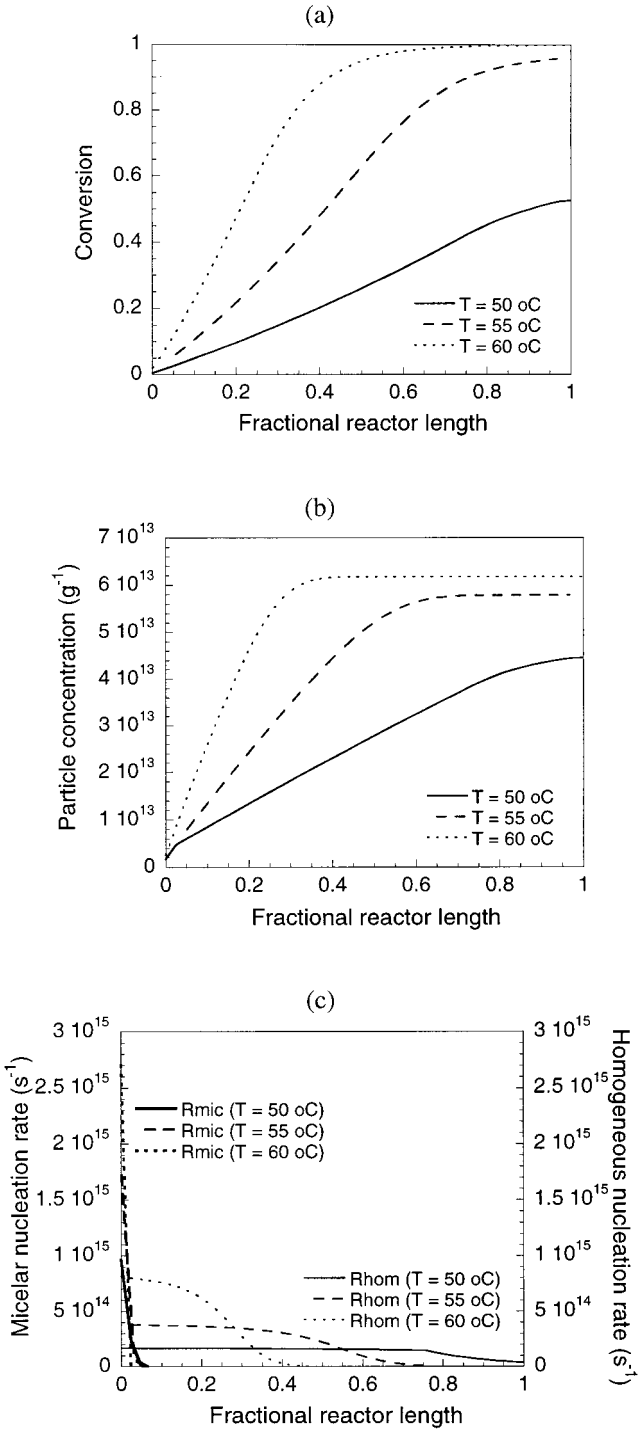

Figure 15. Effect of reaction temperature on the steady-state behavior of continuous vinyl acetate emulsion polymerization reaction in the PSPC: (a) conversion; (b) particle concentration; (c) micellar and homogeneous nucleation rates.

15a, which compares the monomer conversion along the fractional reactor length). Parts b and c of Figure 14 compare the evolution of the particle concentration and average particle diameter. These variables are affected by the reaction temperature in the same way as the polymer fraction: the higher the reaction temperature, the higher the polymer fraction, the particle concentration, and the average particle diameter, with the only exception being the average particle diameters of the reaction at 60 °C that, because of the high particle concentration and high final conversion of this reaction (Figure 15a), were approximately the same as those of the reaction at 55 °C. Parts b and c of Figure 15 compare the steady-state behavior of particle concentration and micellar and homogeneous nucleation rates along the fractional reactor length. While in the reaction at 50 °C the homogeneous nucleation mechanism is active along the whole reator length, leading to an almost

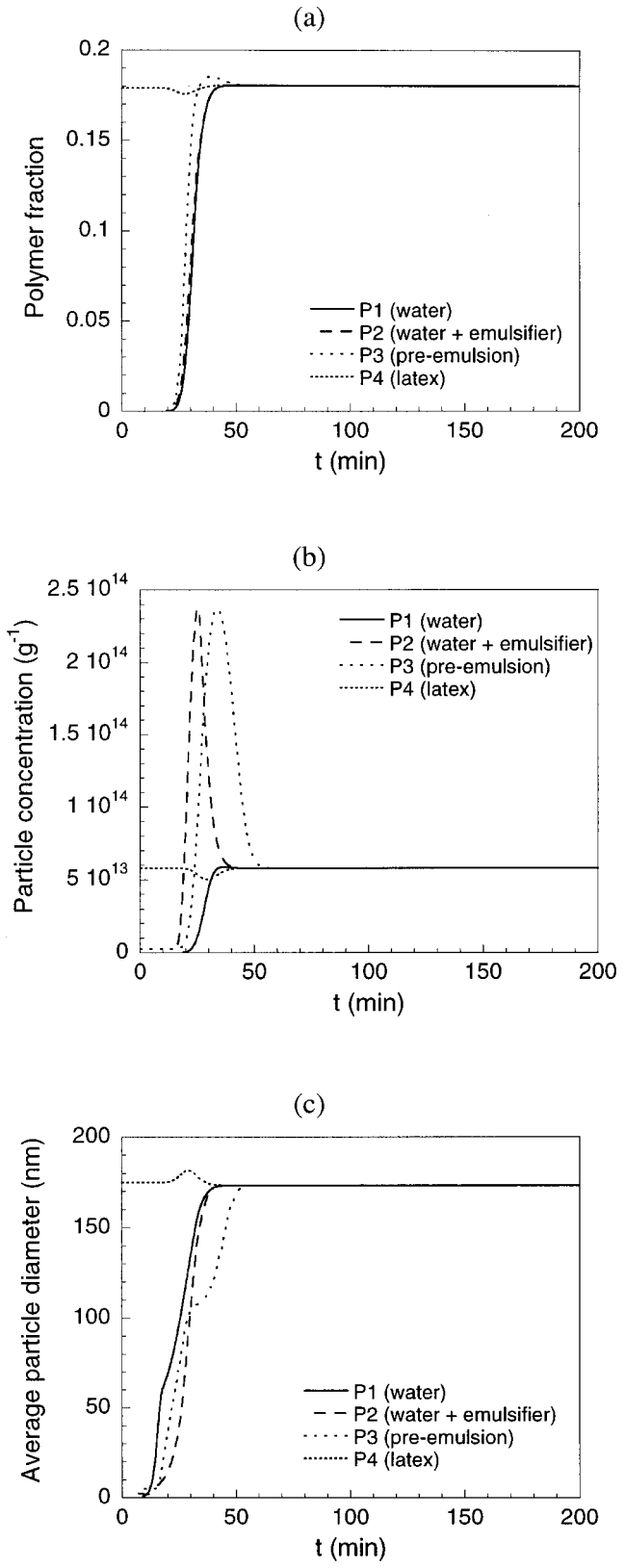

Figure 16. Effect of different start-up procedures on the dynamic behavior of continuous vinyl acetate emulsion polymerization reaction in the PSPC: (a) conversion; (b) particle concentration; (c) average particle diameter.

constant increase of the particle concentration, in the reaction at 60 °C the homogeneous nucleation, although being more intense, is limited to less than half of the reactor length, the point at which the final particle concentration is reached. In all cases the micellar nucleation mechanism was limited to the proximities of the reactor entrance, being faster and more intense at higher reaction temperatures because of the higher initiator decomposition rates.

In sequence four different start-up procedures will be compared: (1) the reactor is filled with water and heated until reaching the reaction temperature (procedure adopted in the experimental run); (2) the reactor is filled with the aqueous phase (water and emulsifier) and heated until reaching the reaction temperature; (3) the reactor is filled with a pre-emulsion composed of monomer, water, emulsifier, and pH buffer and heated until reaching the reaction temperature; (4) the reactor is filled with a latex, with no initiator left, produced under the same conditions and heated until reaching the reaction temperature.

Figure 16 compares the dynamic behavior using those four different start-up procedures. In Figure 16a it might be observed that when using procedure 1 or 2, the behavior of the polymer fraction in the reactor is quite the same. When using procedure 3, in which the reactor is initially filled with pre-emulsion, the increase of the polymer fraction during start-up is slightly faster and a small overshoot might be observed. Finally, when using procedure 4, in which the reactor is initially filled with latex, the polymer fraction is already high at the beginning of the reaction. Parts b and c of Figure 16 compare particle concentrations and average particle diameters. It might be observed that reactions carried out with procedures that involve the presence of emulsifier but no polymer particles in the initial charge of the reactor, like procedures 2 and 3, lead to significant overshoots in the particle concentration (and previous results have shown that this model tends to underestimate this overshoot in the particle concentration). For practical reasons those start-up procedures that might lead to very huge overshoots in the particle concentration should be avoided because very high concentrations of relatively small polymer particles (~100 nm) often lead to very high viscosities and may favor reactor fouling and even plugging.[25] Procedure 3 presented the longest transient period, therefore producing the highest amount of off-specification polymer, as might be observed in Figure 16c. Procedure 4 resulted in the smoothest reactor start-up, as was already observed experimentally by Abad et al.[9] for vinyl acetate/Veova 10 emulsion polymerization reactions performed in a continuous loop reactor. However, procedure 1, besides being fast and not leading to the production of a significant amount of off-specification product, as confirmed experimentally (Figures 4−6), also presents a much smoother start-up behavior than procedures 2 and 3. According to simulation results, under the studied conditions, using different start-up procedures does not lead to different steady-state values in the PSPC.

5. Conclusions

A mathematical model was developed for dynamic simulations of vinyl acetate emulsion polymerizations performed in a new reactor type, the PSPC. The emulsion polymerization model takes micellar and homogeneous nucleation and particle coalescence mechanisms into account. The PSPC is described by an axial dispersion model that allows the simulation of a wide range

of operational conditions. The method of lines was used to discretize the second-order partial differential equations along the axial direction.

The model was capable of reproducing experimental data and provided a feasible explanation on the possible nucleation mechanism during vinyl acetate emulsion polymerization reactions carried out in the PSPC reactor. It was observed that, at the studied operational conditions, the homogeneous nucleation mechanism is very important in order to represent the polymer particle number increase observed experimentally along the reactor length.

The developed model was also used to test different start-up procedures and reaction temperatures, showing that the model is a useful tool in performing simulations in advance of carrying out reactions under new operational conditions.

The future aims of this work include using the developed model in an optimization scheme that computes optimal reactant lateral feed flow rates along the reactor in order to produce polymers with prespecified properties, as well as the experimental implementation of these optimal operational conditions at the PSPC reactor.

Acknowledgment

The financial support from FAPESP (Fundação de Amparo à Pesquisa do Estado de São Paulo) and CNPq (Conselho Nacional de Desenvolvimento Científico e Tecnológico) is gratefully appreciated. The authors also thank Dr. S. Derenzo (IPT) for the particle size analysis.

Nomenclature

a_{col} = length of the PSPC, cm
a_p = superficial area of one polymer particle swollen with monomer, cm^2
a_s = area covered by 1 mol of emulsifier, cm^2/mol
c_c^0 = particle coalescence coefficient, cm^3/s
c_{hom}^0 = coefficient of homogeneous particle nucleation rate
De = axial dispersion coefficient, cm^2/s
D_p = diffusion coefficient in polymer particles, cm^2/s
D_w = diffusion coefficient in the aqueous phase, cm^2/s
[E] = emulsifier concentration in the reactor, mol/cm^3
$[E]_{ads}$ = emulsifier adsorbed on polymer particles per unit surface, mol/cm^2
$[E]^{sat}_{ads}$ = emulsifier per unit surface required to saturate polymer particles, mol/cm^2
$[E]^{aq}$ = emulsifier concentration in the aqueous phase, mol/cm^3
$[E]_{cmc}$ = critical micellar concentration, mol/cm^3
f = initiator efficiency
f_{abs} = absorption efficiency of radicals from the aqueous phase by polymer particles
f^m_{abs} = absorption efficiency of radicals from the aqueous phase by the micelles
f_{void} = void fraction of the PSPC
h = relative term of absorption/termination rates
[I] = initiator concentration in the reactor, mol/cm^3
j_{crit} = critical radical length for homogeneous nucleation
j_z = critical radical length for radical entry into micelles and polymer particles
k = desorption rate coefficient, s^{-1}
k_{0m} = exit rate of a monomeric radical from a polymer particle, s^{-1}
k^m_{abs} = coefficient of the absorption rate of radicals from the aqueous phase by the micelles, $cm^3/mol{\cdot}s$
k_{abs} = coefficient of the absorption rate of radicals from the aqueous phase by polymer particles, $cm^3/mol{\cdot}s$
k_d = decomposition rate constant of the initiator, s^{-1}
k^i_j = partition coefficient between phases i and j
k_f = monomer chain-transfer rate constant, $cm^3/mol{\cdot}s$
k_p = propagation rate constant, $cm^3/mol{\cdot}s$
k_t = termination rate constant, $cm^3/mol{\cdot}s$
m = relative term of desorption/termination rates
[M] = monomer concentration in the reactor, mol/cm^3
$[M]_{aq}$ = monomer concentration in the aqueous phase, mol/cm^3
$[M]_p$ = monomer concentration in polymer particles, mol/cm^3
M_{mic} = number of micelles per volume of the aqueous phase, cm^{-3}
$\bar{n}$ = average number of radicals per polymer particle
N_a = Avogrado's number
N_{mic} = micelle concentration in the reactor, cm^{-3}
N_p = particle concentration in the reactor, cm^{-3}
P = polymer concentration in the reactor, g/cm^3
Pe = Peclet number
PM_m = molecular weight of the monomer, g/mol
q_e = reactor inlet flow rate, cm^3/s
R_1 = concentration of radicals with length 1 in the aqueous phase, mol/cm^3
R_{aq} = concentration of radicals in the aqueous phase, mol/cm^3
r_{col} = internal radius of the PSPC, cm
R_{ent} = concentration of radicals in the aqueous phase that may enter polymer particles, mol/cm^3
$R_{j_{crit}}$ = concentration of radicals presenting critical radical length in the aqueous phase, mol/cm^3
r_m = radius of a micelle, cm
r_p = radius of a polymer particle swollen with monomer, cm
R_{hom} = homogeneous particle nucleation rate, cm^3/s
R_{mic} = micellar particle nucleation rate, cm^3/s
t = time, s
v_{aq} = volume of the aqueous phase, cm^3
v_p = volume of the polymer phase, cm^3
v_R = volume of the reactor, cm^3
v_z = axial velocity, cm/s
z = fractional reactor length
x_{gel} = gel effect function
β_m = probability of a radical in the aqueous phase to react by propagation of by termination
ϕ_w = fraction of water in the reactor
γ = amount of emulsifier per micelle, mol
Ψ = sum of radical propagation and termination rates in the aqueous phase and of the radical absorption rates by micelles and particles, s^{-1}

Literature Cited

(1) Mayer, M. J. J.; Meuldijk, J.; Thoenes, D. Application of the Plug Flow with Axial Dispersion for Continuous Emulsion Polymerization in a pulsed Packed Column. *Chem. Eng. Sci.* **1996**, *51*, 3441−3448.

(2) Greene, R. K.; Gonzales, R. A.; Poehlein, G. W. Continuous Emulsion Polymerization—Steady State and Transient Experiments with Vinyl Acetate and Methyl Methacrylate. In *Emulsion Polymerization*; Piirma, I., Gardon, J. L., Eds.; Washington, DC, 1976.

(3) Kiparissides, C.; MacGregor, J. F.; Hamielec, A. E. Continuous Emulsion Polymerization of Vinyl Acetate. Part I: Experimental Studies. *Can. J. Chem. Eng.* **1980**, *58*, 48−55.

(4) Rawlings, J. B.; Ray, W. R. The Modelling of Batch and Continuous Emulsion Polymerization Reactors: II. Comparison with Experimental Data from Continuous Stirred Tank Reactors. *Polym. Eng. Sci.* **1988**, *28*, 257−274.

(5) Penlidis, A.; MacGregor, J. F.; Hamielec, A. E. Continuous Emulsion Polymerization: Design and Control of CSTR Trains. *Chem. Eng. Sci.* **1989**, *44*, 273−281.

(6) Ohmura, N.; Kataoka, K.; Watanabe, S.; Okubo, M. Controlling Particle Size by Self-Sustained Oscillations in Continuous Emulsion Polymerization of Vinyl Acetate. *Chem. Eng. Sci.* **1998**, *53*, 2129−2135.

(7) Araújo, P. H. H.; de la Cal, J. C.; Asua, J. M.; Pinto, J. C. Modeling Particle Size Distribution (PSD) in Emulsion Copolymerization Reactions in a continuous Loop Reactor. *Macromol. Theory Simul.* **2001**, *10*, 769−779.

(8) Palma, M.; Sayer, C.; Giudici, R. A New Continuous Reactor for Emulsion Polymerization: Effect of Operational Conditions on Conversion and Particle Number. *DECHEMA Monogr.* **2001**, *137*, 625−631.

(9) Palma, M.; Sayer, C.; Giudici, R. Kinetics of Vinyl Acetate Emulsion Polymerizations in a Pulsed Tubular Reactor. Comparison between Experimental and Simulation Results. *Proceedings of III ENPROMER*, Santa Fé, Argentina, Sep 16−20, 2001; Vol. II, pp 889−894.

(10) Lynch, D.; Kiparissides, C. Numerical Simulation of a Tubular Polymerization Reactor. *J. Appl. Polym. Sci.* **1981**, *26*, 1283−1293.

(11) Rollin, A. L.; Patterson, W. I.; Archambault, J.; Bataille, P. Continuous Emulsion Polymerization of Styrene in a Tubular Reactor. *ACS Symp. Ser.* **1979**, *No. 104*, 113.

(12) Paquet, D. A.; Ray, W. H. Tubular Reactors for Emulsion Polymerization: II. Model Comparisons with Experiments. *AIChE J.* **1994**, *40*, 73−87.

(13) Sayer, C.; Giudici, R. Comparison of Different Modeling Approaches for the Simulation of Transient and Steady-State Behaviors of Continuous Emulsion Polymerizations in Pulsed Tubular Reactors. *Braz. J. Chem. Eng.* **2002**, in press.

(14) Hoedemakers, G. F. M. Continuous Emulsion Polymerization in a Pulsed packed Column. Ph.D. Thesis, Eindhoven University of Technology, Eindhoven, The Netherlands, 1990.

(15) Gilbert, R. G. *Emulsion Polymerization*, 1st ed.; Academic Press: London, 1995.

(16) Danckwerts, P. V. Continuous Flow Systems. Distribution of Residence Times. *Chem. Eng. Sci.* **1953**, *2*, 1−13.

(17) Lu, Y. L.; Brooks, Y. J. Effect of Start-up Procedures on the Emulsion Polymerization of Vinyl Acetate in a Continuous-Flow Back-Mixed Reactor. *Chem. Eng. Sci.* **1989**, *44*, 857−871.

(18) Abad, C.; de la Cal, J. C.; Asua, J. M. Start-up Procedures in the Emulsion Copolymerization of Vinyl Esters in a Continuous Loop Reactor. *Polymer* **1995**, *36*, 4293−4299.

(19) Palma, M.; Giudici, R. A New Reactor for Continuous Emulsion Polymerization. Characterization of Flow Non-Ideality. AIChE 2001 Spring National Meeting, Houston, TX, Apr 22−26, 2001.

(20) Casella, E. L. Modelagem Matemática e Estudo Experimental de Sistemas de Polimerização em Emulsão. DSc. Thesis, Escola Politécnica, Universidade de São Paulo, São Paulo, Brazil, 1999 (in Portuguese).

(21) Sayer, C.; Araújo, P. H. H.; Arzamendi, G.; Asua, J. M.; Lima, E. L.; Pinto, J. C. Modeling Molecular Weight Distribution in Emulsion Polymerization Reactions with Transfer to Polymer. *J. Polym. Sci., Part A* **2001**, *39*, 3513−3528.

(22) Melis, S.; Kemmere, M.; Meuldijk, J.; Storti, G.; Morbidelli, M. A Model for the Coagulation of the Polyvinyl Acetate Particles in Emulsion. *Chem. Eng. Sci.* **2000**, *55*, 3101−3111.

(23) Omi, S.; Kushibiki, K.; Negishi, M.; Iso, M. Generalized Computer Modeling of Semi-Batch, n-Component Emulsion Copolymerization Systems and Its Applications. *Zairyo Gijutsu* **1985**, *3*, 426.

(24) Ugelstad, J.; Mork, P. C.; Aasen, J. O. Kinetics of Emulsion Polimerization. *J. Polym. Sci.* **1967**, *5*, 2281−2287.

(25) Araújo, P. H. H. Distribuição de Tamanhos de Partícula em Sistemas Heterogêneos de Polimerização. DSc. Thesis, PEQ-COPPE, Universidade Federal do Rio de Janeiro, Rio de Janeiro, Brazil, 1999 (in Portuguese).

(26) Asua, J. M.; Sudol, E. D.; El Aasser, M. S. Radical Desorption in Emulsion Polymerization. *J. Polym. Sci., Part A* **1989**, *27* (12), 3903−3913.

(27) Forcada, J.; Asua, J. M. Modeling of Unseeded Emulsion Copolymerization of Styrene and Methyl Methacrylate. *J. Polym. Sci., Part A* **1990**, *28* (5), 987−1009.

(28) Petzold, L. R. *A Description of DASSL: a Differential Algebraic System Solver*; Report SAND82-8637; Sandia National Laboratories: Livermore, CA, 1982.

(29) Palma, M.; Miranda, S. C. F.; Sayer, C.; Giudici, R. Comparação Entre Reações Contínuas de Polimerização em Emulsão em uma Coluna Pulsada com Pratos Perfurados com Reações em Batelada. 6° CBPOL, Gramado, Brazil, Nov 11−15, 2001 (in Portuguese).

(30) Hutchinson, R. A.; Paquet, D. A.; McMinn, J. H.; Beuermann, S.; Fuller, R. E.; Jackson, C. *DECHEMA Monogr.* **1995**, *131*, 467.

(31) Chatterjee, A.; Park, W. S.; Graessley, W. W. Free Radical Polymerization with Long Chain Branching: Continuous Polymerization of Vinyl Acetate in t-Butanol. *Chem. Eng. Sci.* **1977**, *32*, 167−178.

(32) Baad, W.; Moritz, H. U.; Reichert, K. H. Kinetics of High Conversion Polymerization of Vinyl Acetate Effects of Mixing and Reactor Type on Polymer Properties. *J. Appl. Polym. Sci.* **1982**, *27*, 2249−2268.

(33) Min, K. W.; Ray, W. H. The Computer Simulation of Batch Emulsion Polymerization Reactors Through a Detailed Mathematical Model. *J. Appl. Polym. Sci.* **1978**, *22*, 89−112.

(34) Unzueta, E.; Forcada, J. Modeling the Effect of Mixed Emulsifier Systems in Emulsion Copolymerization. *J. Appl. Polym. Sci.* **1997**, *66*, 445−458.

(35) Brandrup, J.; Immergut, E. H. *Polymer Handbook*, 3rd ed.; Wiley: New York, 1989.

(36) Perry, R. H.; Chilton, C. H. *Manual de Engenharia Química*, 5th ed.; Guanabara Dois: Rio de Janeiro, Brazil, 1980.

(37) Gardon, J. L. Emulsion Polymerization. II. Review of Experimental Data in the Context of the Revised Smith−Ewart Theory. *J. Polym. Sci., Part A* **1953**, *6*, 643−664.

(38) Unzué, M. J.; Urretabizkaia, A.; Asua, J. M. Maximizing Production Rate and Scrub Resistance of Vinyl Acetate−Veova 10 Latexes. *J. Appl. Polym. Sci.* **2000**, *78*, 475−485.

Received for review August 10, 2001
Revised manuscript received December 26, 2001
Accepted January 7, 2002

IE010675Q